Neuron, Vol. 40, 595–607, October 30, 2003, Copyright ©2003 by Cell Press

Ubiquitination Regulates PSD-95 Degradation and AMPA Receptor Surface Expression

Marcie Colledge,[1,4] Eric M. Snyder,[3,4,5] Robert A. Crozier,[3] Jacquelyn A. Soderling,[1] Yetao Jin,[2] Lorene K. Langeberg,[1] Hua Lu,[2] Mark F. Bear, and John D. Scott[1,*]

[1]Howard Hughes Medical Institute
Vollum Institute
Oregon Health and Science University
Portland, Oregon 97239

[2]Department of Biochemistry and Molecular Biology
Oregon Health and Science University
Portland, Oregon 97239

[3]Howard Hughes Medical Institute
The Picower Center for Learning and Memory
Department of Brain and Cognitive Sciences
Massachusetts Institute of Technology
Cambridge, Massachusetts 02139

Summary

PSD-95 is a major scaffolding protein of the postsynaptic density, tethering NMDA- and AMPA-type glutamate receptors to signaling proteins and the neuronal cytoskeleton. Here we show that PSD-95 is regulated by the ubiquitin-proteasome pathway. PSD-95 interacts with and is ubiquitinated by the E3 ligase Mdm2. In response to NMDA receptor activation, PSD-95 is ubiquitinated and rapidly removed from synaptic sites by proteasome-dependent degradation. Mutations that block PSD-95 ubiquitination prevent NMDA-induced AMPA receptor endocytosis. Likewise, proteasome inhibitors prevent NMDA-induced AMPA receptor internalization and synaptically induced long-term depression. This is consistent with the notion that PSD-95 levels are an important determinant of AMPA receptor number at the synapse. These data suggest that ubiquitination of PSD-95 through an Mdm2-mediated pathway is critical in regulating AMPA receptor surface expression during synaptic plasticity.

Introduction

For synapses to store information, they must exhibit long-lasting changes after their modification by experience. At glutamatergic synapses in the brain, modifications can be triggered by activation of NMDA receptors and expressed as a change in the number of postsynaptic AMPA receptors (Malinow and Malenka, 2002). However, AMPA receptors are rapidly cycled through the postsynaptic membrane under basal conditions (Ehlers, 2000; Lin et al., 2000; Lüscher et al., 1999). For transmission to remain constant in the face of this turnover, it has been suggested that "slot proteins" must exist that reserve insertion sites for AMPA receptors at the synapse (Malinow and Malenka, 2002; Shi et al., 2001). Recruitment of more slot proteins could lead to long-term potentiation (LTP) of synaptic transmission by increasing the postsynaptic capacity for AMPA receptors. Conversely, long-term synaptic depression (LTD) could result from a net loss of slot proteins and their complement of postsynaptic AMPA receptors. Thus, identifying slot proteins and their modes of regulation may provide valuable insight into the molecular basis of information storage by synapses.

One synaptic protein with the properties expected of a slot protein is PSD-95 (Schnell et al., 2002). PSD-95 is attached to the postsynaptic membrane directly by palmitoylation (El-Husseini Ael et al., 2002) and indirectly by PDZ interactions with the cytoplasmic tails of NMDA receptors (Sheng, 2001). PSD-95 also binds to stargazin, a protein that escorts AMPA receptors to the synapse (Chen et al., 2000; Schnell et al., 2002). Via this interaction with stargazin, PSD-95 potentially could act as a docking site for AMPA receptors at the synapse. Consistent with this notion, overexpression of PSD-95 increases the number of AMPA receptors at synapses (El-Husseini et al., 2000; Schnell et al., 2002). Conversely, removal of PSD-95 from the synapse by depalmitoylation depletes synaptic AMPA receptors (El-Husseini et al., 2000).

Recent evidence suggests that the ubiquitin-proteasome pathway regulates many aspects of synaptic function (Hegde and DiAntonio, 2002; Murphey and Godenschwege, 2002). For example, in *C. elegans*, ubiquitination of the glutamate receptor subunit GLR-1 regulates the abundance of synaptic receptors (Burbea et al., 2002). At synapses of *Aplysia* and *Drosophila*, the ubiquitin-proteasome system regulates synaptic strength and growth (DiAntonio et al., 2001; Speese et al., 2003; Zhao et al., 2003). At mammalian synapses, long-term alterations in synaptic activity can affect global changes in the composition of postsynaptic proteins, in part through the ubiquitin-proteasome system (Ehlers, 2003). However, the identity of specific mammalian substrates regulated by ubiquitination during synaptic plasticity remains unknown.

Activation of NMDA receptors on hippocampal neurons can cause a net loss of synaptic AMPA receptors and stable LTD (Carroll et al., 1999; Ehlers, 2000; Heynen et al., 2000; Lee et al., 1998; Liao et al., 1999; Man et al., 2000). These changes might be caused by reduced synaptic expression of slot proteins. We therefore examined whether PSD-95 expression at the synapse is altered by brief NMDA receptor activation. Here we report that NMDA treatment leads to ubiquitination of PSD-95 and subsequent degradation by the 26S proteasome. Like LTD and AMPA receptor internalization, this process requires calcium-dependent dephosphorylation of PKA substrates. Two lines of evidence suggest that regulation of PSD-95 levels by the ubiquitin-proteasome system is an important regulator of synaptic transmission and plasticity. First, we find that NMDA-induced endocytosis of AMPA receptors is blocked by a mutation

*Correspondence: scott@ohsu.edu
[4]These authors contributed equally to this work.
[5]Present address: The Laboratory for Cellular and Molecular Neuroscience, Rockefeller University, New York, New York 10021.

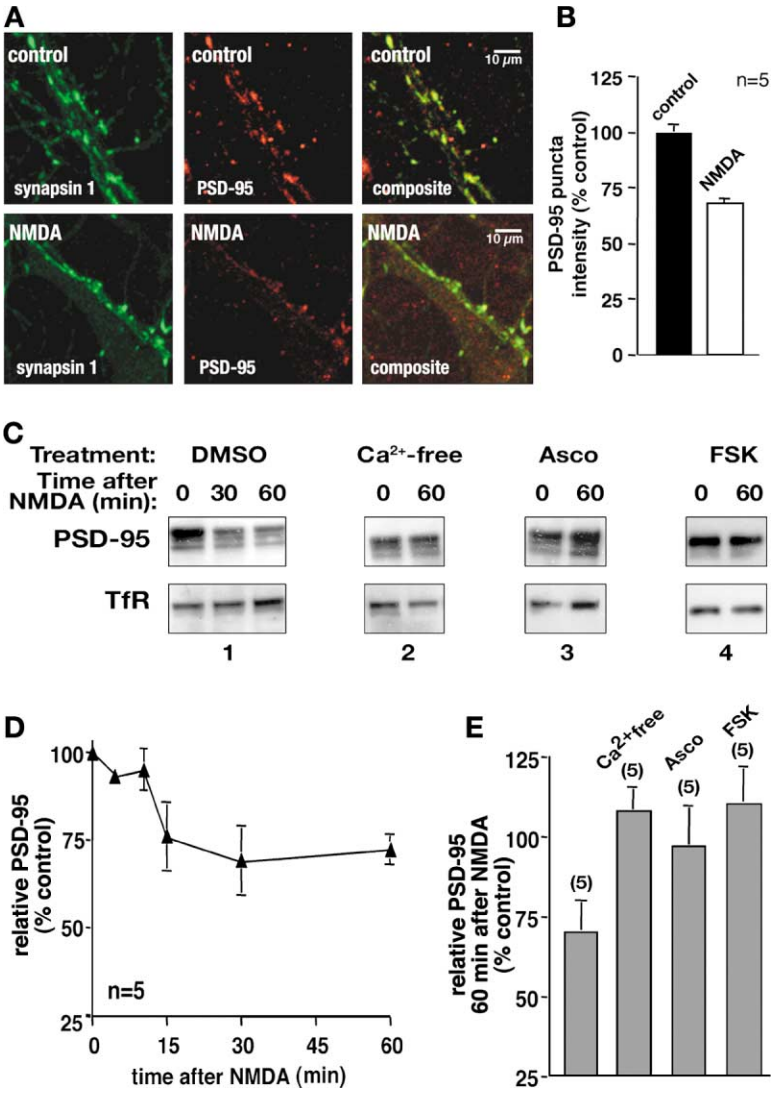

Figure 1. NMDA Treatment Causes Loss of PSD-95 from Synapses and a Reduction in Total Cellular PSD-95

(A) In the absence of NMDA treatment (upper panels), PSD-95 (red) colocalizes with synapsin 1 (green) at synapses. In the composite, colocalized synapsin and PSD-95 puncta appear yellow. Thirty minutes following NMDA treatment (20 μM, 3 min; bottom panels), synaptic staining for PSD-95 was reduced, without affecting synapsin immunoreactivity. Following NMDA stimulation, the overlay image of PSD-95 and synapsin immunoreactivity is dominated by green synapsin staining.

(B) Quantification revealed that, following NMDA treatment, the intensity of PSD-95 was reduced to 67% ± 4% of control levels (n = 250 synapses from ten cells in four cultures).

(C) NMDA treatment causes a loss of total cellular PSD-95. (Panel 1) In control conditions (DMSO), hippocampal neurons were stimulated with NMDA (20 μM, 3 min); cells were lysed 30 or 60 min later, and total levels of PSD-95 and transferrin receptor were analyzed. NMDA caused a rapid and long-lasting loss of total PSD-95 (top panel); total levels of transferrin receptor were unchanged (TfR; bottom panel). (Panel 2) Reduction in PSD-95 levels did not occur in calcium-free (Ca^{2+}-free) media. (Panel 3) Treatment with the PP2B antagonist ascomycin (Asco; 2 μM) prevented loss of PSD-95. (Panel 4) The adenylyl cyclase activator forskolin (FSK; 50 μM) also prevented loss of PSD-95.

(D) NMDA stimulation causes a rapid reduction in relative PSD-95 levels (PSD-95/TfR levels) that is maintained for at least 60 min (n = 5).

(E) Quantification of several experiments 60 min following NMDA treatment. NMDA-induced reduction in PSD-95 levels was blocked in calcium-free media (Ca^{2+}-free; n = 4). PSD-95 loss did not occur in the presence of the PP2B inhibitor ascomycin (Asco; n = 5) or the adenylyl cyclase activator forskolin (FSK; n = 5). For each condition, statistical comparisons were made to the appropriate vehicle control.

that prevents ubiquitination of PSD-95. Second, we show that inhibiting the proteasome, which blocks PSD-95 degradation, prevents NMDA-induced internalization of AMPA receptors and reduces synaptically induced LTD. These data suggest that the ubiquitin-proteasome system regulates the molecular architecture of glutamatergic synapses and plays a key role in synaptic plasticity in the mammalian brain.

Results

Activation of NMDA Receptors Reduces PSD-95 Protein Levels

Brief exposure of cultured hippocampal neurons or acutely prepared hippocampal slices to NMDA stimulates internalization of AMPA receptors and LTD of synaptic transmission (Beattie et al., 2000; Ehlers, 2000; Lee et al., 1998; Lu et al., 2001). To investigate the fate of PSD-95 following NMDA receptor activation, we labeled cultured hippocampal neurons for the synaptic marker synapsin 1 (green) and PSD-95 (red; Figure 1A). In control cultures, PSD-95 extensively colocalized with synapsin (Figure 1A, upper panel). However, following NMDA stimulation (20 μM, 3 min), the intensity of PSD-95 puncta was reduced to 67% ± 4% of control levels ($p < 0.01$; n = 250 synapses from ten cells in four cultures; Figure 1A, bottom panel; Figure 1B). These data suggest that NMDA treatment causes a rapid loss of PSD-95 from synaptic sites.

To further examine this phenomenon, we measured the total cellular levels of PSD-95 following NMDA stimulation. PSD-95 protein levels were assessed by Western blot and quantified by densitometry. NMDA caused a reduction in total PSD-95 levels by 15 min that was maintained for at least 60 min (72% ± 5% of control levels, $p < 0.05$, n = 5; Figure 1C, upper panel 1 and Figure 1D). In contrast, NMDA caused no decrease in the levels of the transferrin receptor (Figure 1C, lower panel 1), tubulin, or actin (data not shown).

Calcium influx through the NMDA receptor is known to regulate many synaptic events, including LTD (Bear and Malenka, 1994). To test whether it is required for

the loss of cellular PSD-95, we repeated the experiments in calcium-free media. In the absence of external calcium, NMDA-induced loss of PSD-95 was blocked (105% ± 4% of control levels, $p > 0.3$, $n = 5$; Figure 1C, panel 2, and Figure 1E).

Calcium entry induces LTD by activation of the phosphatase PP2B (calcineurin; Mulkey et al., 1994). We hypothesized that PP2B also may serve as a calcium sensor in the downregulation of PSD-95 protein levels. To test this, we repeated experiments in the presence of the potent and specific PP2B inhibitor ascomycin (Asco; 2 μM), an analog of FK-506 (Liu et al., 1991). Inhibition of PP2B prevented the NMDA-induced loss of PSD-95 (97% ± 4%, $p > 0.4$, $n = 5$; Figure 1C, panel 3, and Figure 1E). Together, these data suggest that PP2B is required for the NMDA-induced loss of PSD-95.

PP2B can regulate synaptic strength through the dephosphorylation of protein kinase A (PKA) substrates (Beattie et al., 2000; Kameyama et al., 1998; Lee et al., 1998; Mulkey et al., 1994; Tavalin et al., 2002; Zeng et al., 2001). We therefore hypothesized that the PKA pathway may be involved in the loss of PSD-95. To test this, we pretreated cultures with the adenylyl cyclase activator forskolin (FSK; 50 μM, 30 min) prior to application of NMDA. Forskolin prevented the reduction of PSD-95 levels (110% ± 12% of control levels, $p > 0.2$, $n = 5$; Figure 1C, panel 4, and Figure 1E). These data indicate that the cAMP/PKA pathway is involved in regulating PSD-95 levels.

PSD-95 Is Ubiquitinated in Response to Activation of NMDA Receptors

Recent work has shown that PDZ domain-containing proteins are regulated by the ubiquitin pathway (Gardiol et al., 1999; Glaunsinger et al., 2000; Lee et al., 2000b). Ubiquitin is a 76 amino acid protein that is covalently attached to substrate proteins. Once tagged with ubiquitin, substrate proteins are often targeted for rapid degradation by the 26S proteasome (Weissman, 2001). We therefore hypothesized that NMDA receptor activation may lead to a loss of PSD-95 via degradation by the ubiquitin-proteasome pathway. To test this, we treated cultured hippocampal neurons with NMDA (20 μM, 3 min), immunoprecipitated PSD-95 at different time points, and immunoblotted the samples for ubiquitin. We observed a rapid and transient increase in ubiquitination of PSD-95 that peaked approximately 10 min following NMDA treatment (Figure 2A, top panel). As these experiments were performed under nondenaturing conditions, it is possible that the ubiquitin-positive bands represent a coprecipitating protein that associates with PSD-95. However, the higher molecular weight ubiquitinated species also were recognized specifically by PSD-95 antibodies, suggesting that they are indeed ubiquitinated forms of PSD-95 (Supplemental Figure S1 available at http://www.neuron.org/cgi/content/full/40/3/595/DC1). Control experiments confirmed that equivalent amounts of PSD-95 were immunoprecipitated in each condition (Figure 2A, bottom panel). Examination of total cell extracts showed a loss of total PSD-95 protein following the NMDA treatment (Figure 2B), consistent with our earlier results. These data indicate that NMDA receptor activation leads to rapid and transient ubiquitination of PSD-95. However, we are unable to establish at this time whether this represents polyubiquitination or monoubiquitination on multiple sites.

To test the specificity of this effect, we repeated these experiments under identical conditions and immunoprecipitated GluR2-containing AMPA receptor complexes following NMDA treatment. We saw no evidence for ubiquitination of GluR2 receptors following NMDA stimulation (Figure 2C, upper panel), although control experiments confirmed that GluR2 was efficiently immunoprecipitated (Figure 2C, bottom panel). These data suggest that NMDA treatment induces the selective ubiquitination of PSD-95.

PEST sequences are known to regulate ubiquitination and rapid protein turnover (Rechsteiner and Rogers, 1996). The PEST-FIND program (www.at.embnet.org/embnet/tools/bio/PESTfind) predicts that PSD-95 contains a PEST sequence at its N terminus (amino acids 13–23 in rat PSD-95; Figure 2D). To determine if this region in PSD-95 is important for its ubiquitination, we generated a deletion mutant lacking this region—PSD-95ΔPEST. HEK293 cells were transfected with HA-tagged ubiquitin and PSD-95ΔPEST or wild-type PSD-95. Ubiquitination of PSD-95ΔPEST was dramatically reduced compared to wild-type PSD-95 (Figure 2E, top panel, lanes 2 and 3), although equivalent amounts of both proteins were immunoprecipitated (Figure 2E, bottom panel). These data suggest that the PEST sequence in PSD-95 is critical for its ubiquitination.

PSD-95 Is Associated with the Ubiquitin E3 Ligase Mdm2

Ubiquitination involves the sequential action of three enzymes: the ubiquitin-activating enzyme (E1), a ubiquitin-conjugating enzyme (E2), and a ubiquitin ligase (E3; Joazeiro and Hunter, 2000). Specificity is determined by the E3 ligases, which specifically interact with their protein substrates. As a further step toward understanding a role for ubiquitination in regulating PSD-95, we sought to identify its E3 ligase partner. Toward this end, we immunoprecipitated four candidate ligases—Mdm2, E6AP, Parkin, and Cbl—from synaptic plasma membranes (Figure 3A). Each immune complex was screened for copurification of PSD-95 by immunoblot. PSD-95 was detected only in Mdm2 immunoprecipitates (Figure 3A, lane 6) but not in control IgG, E6AP, Parkin, or Cbl complexes (Figure 3A, lanes 2–5). Control experiments confirmed that each antibody did indeed immunoprecipitate its appropriate antigen (data not shown). In reciprocal experiments, Mdm2 copurified with PSD-95 (Figure 3B, lane 3) but not with control IgG (Figure 3B, lane 2). In addition, neither E6AP, Parkin, nor Cbl copurified with PSD-95 (data not shown). Collectively, these data provide strong evidence that PSD-95 and Mdm2 interact in synaptic membranes.

To extend our biochemical data, we examined the subcellular distribution of Mdm2 in cultured hippocampal neurons by immunocytochemistry (Figure 3C). Mdm2 (red) staining was predominantly punctate and colocalized with the synaptic marker synapsin 1 (green) at many sites (Figure 3, upper panels). This was more evident at higher magnification (Figure 3, lower panels). Mdm2 was present at 64% ± 5% of synapsin puncta

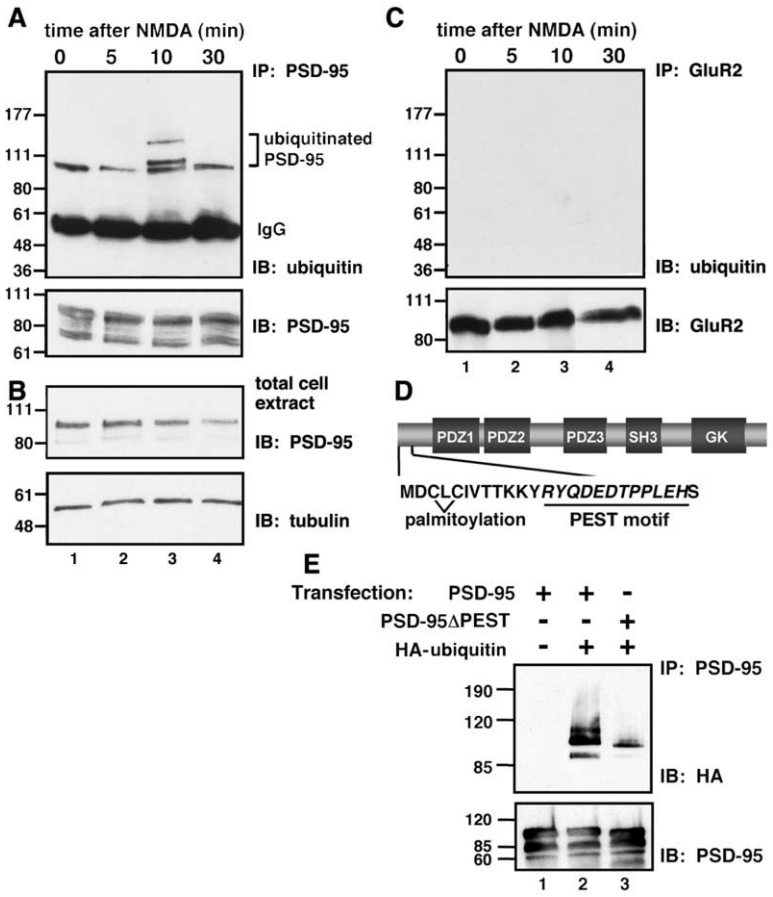

Figure 2. NMDA Treatment Causes Ubiquitination of PSD-95 that Depends on a PEST Motif

(A) NMDA stimulates ubiquitination of PSD-95 in cultured hippocampal neurons. Hippocampal neurons were treated with NMDA (20 μM, 3 min) and lysed at various times following treatment. PSD-95 was immunoprecipitated, and samples were immunoblotted with ubiquitin antibodies. NMDA treatment caused rapid ubiquitination of PSD-95 that peaked at 10 min (upper panel, lane 3). Equivalent amounts of PSD-95 were precipitated in each condition (lower panel).

(B) NMDA treatment causes a loss of total PSD-95 from neuron extracts by 30 min (upper panel; consistent with Figure 1C). NMDA did not affect levels of the loading control tubulin (lower panel).

(C) NMDA treatment does not stimulate ubiquitination of GluR2 AMPA receptors. The same conditions that caused ubiquitination of PSD-95 failed to stimulate ubiquitination of GluR2 (upper panel), although GluR2 was efficiently immunoprecipitated (lower panel).

(D) Cartoon of PSD-95 showing its modular domain structure. PSD-95 contains three PDZ domains, an SH3 domain, and a guanylate kinase (GK)-like region. At its N terminus, PSD-95 contains a PEST motif (italicized). PSD-95ΔPEST lacks this sequence but retains the palmitoylation sites (cysteines indicated).

(E) Ubiquitination of PSD-95 requires the PEST motif. HEK293 cells were transfected with myc-tagged PSD-95 alone (lane 1), together with HA-tagged ubiquitin (lane 2), or with a mutant form of PSD-95 lacking the PEST sequence motif (PSD-95ΔPEST) and HA-ubiquitin (lane 3). Wild-type PSD-95 was ubiquitinated (top panel; lane 2), whereas ubiquitination of PSD-95ΔPEST was dramatically reduced (top panel, lane 3). Reprobing the blot with antibodies against PSD-95 showed that equivalent amounts of PSD-95 were precipitated in each case (bottom panel).

(n = 250 synapses from four cultures). These data indicate that Mdm2 is found at a majority of synapses in hippocampal neurons.

PSD-95 Is Ubiquitinated by Mdm2

To test directly whether PSD-95 is a substrate for Mdm2, we performed in vitro ubiquitination assays (Figure 4A). GST-PSD-95 showed a laddering of higher molecular weight ubiquitinated species when all components of the ubiquitination machinery were present (Figure 4A, top panel, lane 4). On shorter exposure, we confirmed that equivalent amounts of GST-PSD-95 were used in each condition (Figure 4A, bottom panel). Parallel, positive control experiments confirmed that p53, a well-studied substrate for Mdm2, exhibited a similar laddering of ubiquitinated species (data not shown). These data indicate that PSD-95 can indeed be ubiquitinated by Mdm2.

Mdm2 activity can be specifically inhibited by the cellular protein p14/19ARF (Sherr and Weber, 2000). If Mdm2 is important for degradation of PSD-95, then we would predict that p14ARF would block this. We cotransfected HEK293 cells (which endogenously express Mdm2) with PSD-95 and p14ARF (Figure 4B). In the presence of p14ARF, we observed a significant increase in total PSD-95 levels (Figure 4B, upper panel, lane 2), relative to vector-transfected controls (Figure 4B, upper panel, lane 1). Cotransfection of p14ARF increased PSD-95 levels to 176% ± 23% of controls (Figure 4C; $p < 0.05$, $n = 3$). As a control, we cotransfected GFP; p14ARF had no effect on GFP levels (Figure 4B, bottom panel). We next tested whether the PEST sequence in PSD-95 is important for regulation by Mdm2. In contrast to wild-type PSD-95, PSD-95ΔPEST levels were not increased by cotransfection with p14ARF (Figure 4B, lanes 3 and 4, and Figure 4C; p14ARF levels were 115% ± 17% of vector-transfected controls, $p > 0.2$, $n = 3$), indicating that the PEST sequence is important for the Mdm2-mediated degradation of PSD-95.

As a corollary to these experiments, we asked whether overexpression of Mdm2 reduces total levels of PSD-95 (Figures 4D and 4E). We found that cotransfection of Mdm2 reduced levels of PSD-95 to 56% ± 2% of control levels (Figure 4D, lanes 1 and 2, and Figure 4E; $p < 0.05$, $n = 3$). Overexpression of Mdm2 did not affect levels of PSD-95ΔPEST (Figure 4D, lanes 3 and 4).

Finally, we examined ubiquitination of PSD-95 in cells from mice lacking Mdm2 (Montes de Oca Luna et al., 1995). *Mdm2*$^{-/-}$ mouse embryonic fibroblasts were transfected with PSD-95, HA-tagged ubiquitin, and Mdm2 (Figure 4F). In the absence of Mdm2, PSD-95 was not ubiquitinated (Figure 4F, top panel, lane 1). In contrast,

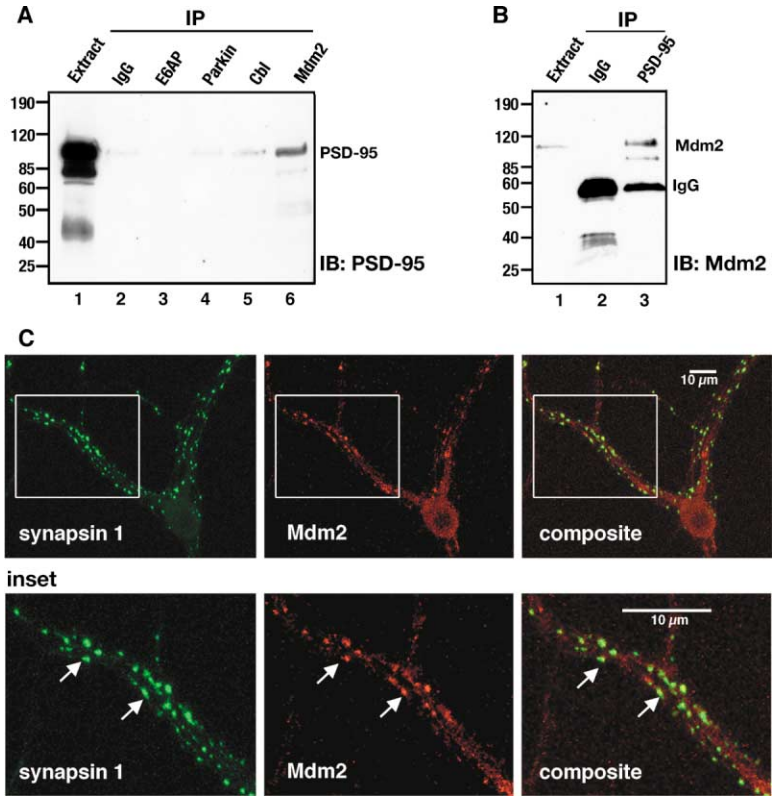

Figure 3. PSD-95 Associates with Mdm2, a Ubiquitin E3 Ligase

(A) PSD-95 copurifies with Mdm2. Extracts of synaptic plasma membranes were subjected to immunoprecipitation using antibodies against several ubiquitin E3 ligases (lanes 2–6). PSD-95 copurified with Mdm2 (lane 6) but not with control nonimmune IgG, E6AP, Parkin, or Cbl. Extract (lane 1) represents 1% of amount used in immunoprecipitation.

(B) Mdm2 copurifies with PSD-95. Synaptic plasma membrane extracts were immunoprecipitated with antibodies against PSD-95. Mdm2 specifically copurified in PSD-95 precipitates (lane 3) but not in control IgG precipitates (lane 2). Extract (lane 1) represents 10% of total used in immunoprecipitation.

(C) Mdm2 is localized at synapses. (Upper panel) Cultured hippocampal neurons were labeled with anti-synapsin 1 antibodies (green) to mark synaptic sites and Mdm2 antibodies (red). Overlay demonstrates that Mdm2 immunoreactivity is present at a majority of synapses. (Lower panel) Higher-magnification view (corresponding to region marked by boxes in upper panel) shows that 64% ± 5% (n = 250 synapses from four cultures) of synapsin 1-positive sites are immunoreactive for Mdm2. Examples of synapses positive for both synapsin 1 and Mdm2 are indicated with arrows.

PSD-95 was ubiquitinated in rescue experiments in which Mdm2 was transfected back into these cells (Figure 4F, top panel, lane 2). In comparison, ubiquitination of PSD-95ΔPEST was greatly reduced (Figure 4F, lanes 3 and 4), although similar amounts of PSD-95 and PSD-95ΔPEST were immunoprecipitated (Figure 4F, bottom panel). Collectively, the data in Figure 4 strongly support the notion that Mdm2 is required for ubiquitination and degradation of PSD-95 and that the PEST sequence is critical in this process.

The Proteasome Regulates PSD-95 Levels

Following ubiquitination, substrate proteins are often targeted to the 26S proteasome for degradation (Pickart, 2000). To test whether the proteasome is involved in the NMDA-induced degradation of PSD-95, we treated primary hippocampal neuron cultures with the cell-permeable proteasomal inhibitor MG132 (50 μM, 1 hr), prior to NMDA stimulation (20 μM, 3 min). As before, NMDA alone induced a loss of total PSD-95 protein (Figures 5A and 5C; 60% ± 15% of DMSO control, $p < 0.05$, $n = 5$). In contrast, MG132 completely blocked this effect (Figures 5B and 5C; 110% ± 14% of MG132 alone, $p > 0.2$, $n = 5$). The structurally distinct proteasomal inhibitor lactacystin also blocked the NMDA-induced degradation of PSD-95 (Supplemental Figure S2 at http://www.neuron.org/cgi/content/full/40/3/595/DC1). These data suggest that, following NMDA stimulation, ubiquitinated PSD-95 is degraded by the 26S proteasome.

The Proteasome Regulates Surface AMPA Receptors

If PSD-95 determines the capacity of the synaptic membrane for AMPA receptors, as has been hypothesized (Schnell et al., 2002), then treatments that inhibit proteasomal degradation of PSD-95 also should interfere with NMDA-induced loss of surface AMPA receptors. To test this, we measured surface expression of AMPA receptors using a biotinylation assay (Snyder et al., 2001). We found that NMDA treatment (20 μM, 3 min) caused a long-lasting loss of surface GluR1 (Figures 5D and 5F; 60% ± 5% of control levels at 60 min, $p < 0.05$; $n = 6$). There was no change in surface levels of transferrin receptors (Figure 5F). In the presence of MG132, however, the NMDA-induced loss of surface GluR1 was completely blocked (Figures 5E and 5G; 104% ± 5% of control levels at 60 min, $p > 0.4$, $n = 7$). These data indicate that inhibiting proteasome activity, which blocks degradation of PSD-95, prevents the loss of surface AMPA receptors following NMDA receptor activation.

We next used immunocytochemistry to visualize changes in surface-expressed, synaptic AMPA receptors (Figures 5H–5K). NMDA (20 μM, 3 min) caused a loss of synaptic GluR2 (Figures 5H, 5I, and 5L; intensity of GluR2 puncta was 55% ± 11% of controls; $p < 0.05$, $n = 10$). In contrast, pretreatment with MG132 (50 μM, 30 min) significantly blocked the NMDA-induced loss of surface GluR2 (Figures 5K and 5L; 82% ± 16% of DMSO, $p < 0.05$, $n = 10$ cells). These data further support a role for the proteasome in regulating AMPA receptor surface expression.

Ubiquitination of PSD-95 Regulates Endocytosis of AMPA Receptors

To test directly if ubiquitination of PSD-95 regulates AMPA receptor internalization, we transfected cultured hippocampal neurons with PSD-95ΔPEST, which is de-

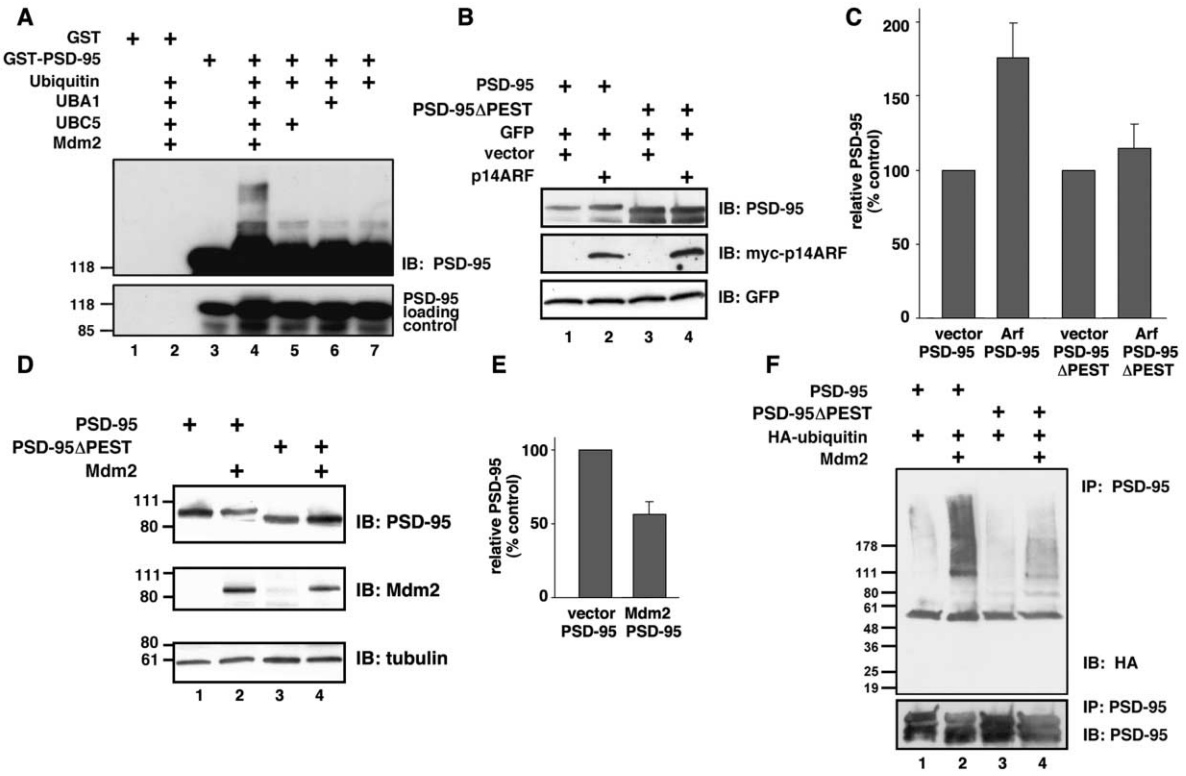

Figure 4. Mdm2 Ubiquitinates PSD-95 and Regulates Its Expression Levels

(A) Mdm2 directly ubiquitinates PSD-95. GST-PSD-95 was incubated with ubiquitin (Ub), E1 (UBA1), E2 (UBC5), and Mdm2 (E3; lanes 3–7). Ubiquitination was detected using PSD-95 antibodies. GST-PSD-95 showed a laddering of higher molecular weight ubiquitinated species when the full complement of the ubiquitination machinery was present (upper panel; lane 4). Equal amounts of GST-PSD-95 were used in each reaction (lower panel).

(B) p14ARF stabilizes cellular levels of PSD-95. HEK293 cells were transfected with either myc-tagged PSD-95 (lanes 1 and 2) or PSD-95ΔPEST (lanes 3 and 4) and GFP, in the absence or presence of myc-tagged p14ARF, a cellular inhibitor of Mdm2 activity. In the presence of p14ARF, levels of PSD-95 protein in total cellular extracts were increased (upper panel; compare lanes 1 and 2). p14ARF did not affect levels of PSD-95ΔPEST (lane 4) nor of cotransfected GFP (bottom panel).

(C) Quantification of p14ARF effect. p14ARF increases the levels of wild-type PSD-95 to 176% ± 23% of control levels ($p < 0.05$, $n = 3$) but does not alter levels of PSD-95ΔPEST (115% ± 17% of controls, $p > 0.2$, $n = 3$).

(D) Mdm2 reduces total PSD-95 levels. HEK293 or H1299 cells were transfected with myc-tagged PSD-95 (lanes 1 and 2) or PSD-95ΔPEST (lanes 3 and 4) in the absence and presence of Mdm2. In the presence of Mdm2, levels of PSD-95 protein in total cell extracts were reduced (upper panel, lane 2). Expression of Mdm2 had no effect on levels of PSD-95ΔPEST (upper panel, lane 4). Equivalent amounts of extracts were loaded in each condition (tubulin; bottom panel).

(E) Quantification of Mdm2 effect. Expression of Mdm2 decreases levels of PSD-95 to 56% ± 9% of control levels ($p < 0.05$, $n = 3$).

(F) In the absence of Mdm2, PSD-95 is not ubiquitinated. Mouse embryonic fibroblasts lacking Mdm2 (*Mdm2*$^{-/-}$), were transfected with myc-tagged PSD-95 (lanes 1 and 2) or PSD-95ΔPEST (lanes 3 and 4) and HA-ubiquitin, with or without Mdm2. Cells were lysed, and PSD-95 was immunoprecipitated. Only when Mdm2 was reintroduced into the cells was PSD-95 ubiquitinated (upper panel, lane 2). Mdm2-mediated ubiquitination of PSD-95ΔPEST was greatly reduced (upper panel, lane 4). Equivalent amounts of PSD-95 were immunoprecipitated in all conditions (bottom panel).

fective in its ability to be ubiquitinated. An antibody feeding protocol was used to measure AMPA receptor endocytosis following NMDA treatment (Figure 6; Ehlers, 2000; Lin et al., 2000). Using this method, we were able to monitor both surface and internal pools of AMPA receptors. In control, untransfected cells (left panels), NMDA treatment (+) caused internalization of GluR2. This was measured as a loss in the density of surface GluR2 puncta (Figures 6A and 6B; red, left panels; Figure 6C; control: 2.6 ± 0.6 puncta/10 μm; NMDA: 1.9 ± 0.3 puncta/10 μm; $p < 0.02$, $n = 16$) and an increase in the density of internal GluR2 puncta (Figures 6A and 6B; green; Figure 6D; control: 0.44 ± 0.1 puncta/10 μm; NMDA: 2.1 ± 0.15 puncta/10 μm, $p < 0.01$, $n = 16$). As we hypothesized, transfection of PSD-95ΔPEST (middle panels) blocked both the NMDA-induced loss of surface AMPA receptors (Figures 6A and 6B; red, middle panels; Figure 6C; control: 3.6 ± 0.34 puncta/10 μm; NMDA: 3.25 ± 0.2 puncta/10 μm, $p > 0.09$, $n = 15$) and the increase in internalized receptors (Figure 6A, green; Figure 6D; control: 0.33 ± 0.2 puncta/10 μm; NMDA: 0.68 ± 0.17 puncta/10 μm; $p > 0.15$, $n = 15$). These data indicate that overexpression of PSD-95ΔPEST reduces NMDA-stimulated AMPA receptor endocytosis, suggesting that ubiquitination of PSD-95 is necessary for efficient internalization of AMPA receptors. These results are more clearly illustrated in higher-magnification views of the neuronal dendrites (Figure 6B).

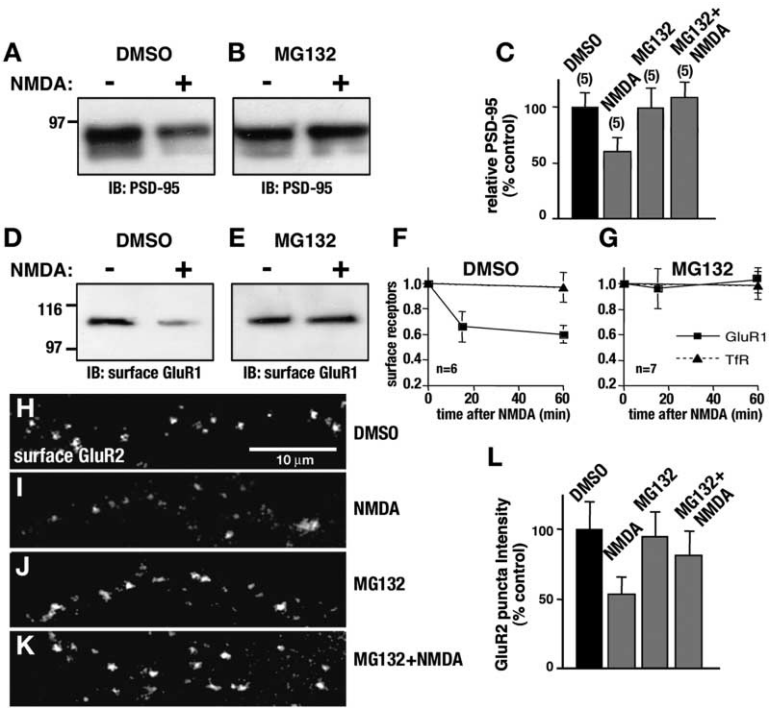

Figure 5. The Proteasome Regulates PSD-95 Degradation and Surface AMPA Receptor Expression

(A) Under control conditions, NMDA (20 μM, 3 min) causes a loss of total PSD-95 protein in hippocampal neurons (+).

(B) MG132 prevents NMDA-induced degradation of PSD-95. Cultures were treated with MG132 (50 μM, 1 hr) prior to NMDA stimulation. Inhibiting the proteasome with MG132 blocks this NMDA-induced degradation of PSD-95 (+). The proteasomal inhibitor lactacystin also blocked PSD-95 degradation (data not shown).

(C) Quantification of PSD-95 levels. NMDA causes degradation of PSD-95 (60% ± 15% of controls; n = 5). MG132 prevents this effect (110% ± 14% of MG132 alone; n = 5).

(D) NMDA causes loss of surface AMPA receptors. Cultures were treated with DMSO (1 hr) and then stimulated with NMDA (20 μM, 3 min). One hour following NMDA treatment, the cultures were biotinylated, and surface proteins were precipitated with neutravidin sepharose. NMDA treatment caused a loss of surface GluR1 (+).

(E) MG132 prevents NMDA-induced loss of surface AMPA receptors. Cultures were incubated in MG132 (50 μM, 1 hr) prior to NMDA (20 μM, 3 min) treatment, and surface receptors were isolated 1 hr later. NMDA-induced loss of surface GluR1 was blocked by MG132 (+; right lane).

(F) Quantification reveals that NMDA reduces surface GluR1 by 30% within 15 min and that this effect lasts at least 1 hr. There was no change in levels of transferrin receptor (TfR) over this time.

(G) In MG132, NMDA-induced changes in surface GluR1 are blocked. There was no change in levels of transferrin receptor (TfR).

(H–K) Hippocampal cultures were pretreated with MG132 (50 μM, 30 min) prior to NMDA stimulation (20 μM, 3 min). Fifteen minutes later, surface GluR2 receptors were labeled. NMDA caused a reduction in surface GluR2 staining. MG132 blocked this effect.

(L) Following NMDA treatment, the intensity of GluR2 puncta was 55% ± 11% of controls (n = 10 cells from four cultures). MG132 largely blocked the NMDA-induced loss of surface GluR2 (82% ± 16% of controls; n = 10 cells from four cultures).

We also examined neurons transfected with wild-type PSD-95 (Figure 6A, right panels). NMDA-induced endocytosis of AMPA receptors was blunted in PSD-95-expressing neurons compared to control neurons; however, endocytosis was greater than in PSD-95ΔPEST neurons. In PSD-95-expressing neurons, NMDA treatment caused a reduction in surface GluR2 puncta density (Figure 6C; control: 3.5 ± 0.26 puncta/10 μm; NMDA: 2.6 ± 0.3 puncta/10 μm, $p < 0.05$, n = 16) and an increase in internal GluR2 puncta density (Figure 6D; control: 0.36 ± 0.37 puncta/10 μm; NMDA: 1.44 ± 0.16 puncta/10 μm, $p < 0.05$, n = 16). Higher-magnification views (Figure 6B, right) illustrate these effects. These results suggest that overexpression of PSD-95 can partially reduce the effect of NMDA on AMPA receptor endocytosis, consistent with a role for PSD-95 in stabilizing surface AMPA receptors. Together, these data indicate that PSD-95 plays a direct role in regulating AMPA receptor trafficking and that ubiquitination of PSD-95 is required for AMPA receptor endocytosis.

The Proteasome Regulates Hippocampal LTD

Finally, we tested whether proteasomal degradation of PSD-95 might be an underlying mechanism for the activity-dependent removal of glutamate receptors during LTD. We isolated hippocampal slices from young rats and performed whole-cell voltage-clamp recordings of CA1 neurons intracellularly perfused with vehicle, MG132, or lactacystin. LTD was reliably induced in vehicle control cells using a pairing protocol (Figures 7A and 7B; 52% ± 10% reduction relative to baseline responses). In contrast, inhibition of proteasome activity by MG132 significantly attenuated LTD (Figures 7A and 7B; 78% ± 5% of baseline responses, $p < 0.03$). MG132 itself had no effect on basal synaptic transmission (data not shown). To confirm a role for the proteasome in this process, we repeated the experiments with the structurally distinct proteasome inhibitor lactacystin. Lactacystin also blocked LTD (Figures 7C and 7D; 95% ± 14% of baseline responses, $p < 0.05$). Together these data suggest a role for the proteasome in the regulation of synaptic depression.

Discussion

Although the postsynaptic density (PSD) appears rigid and insoluble, it is a dynamic structure and the site of continual plasticity. We show here that the levels of PSD-95, a major organizer of the PSD, are regulated by ubiquitination. This process is signaled through NMDA receptor activation, which induces ubiquitination of PSD-95 and its removal from synaptic sites by degradation. Loss of PSD-95 presumably untethers AMPA receptors from the postsynaptic membrane, allowing for their subsequent removal from synaptic sites by endocytosis. We propose that through rapid and dynamic

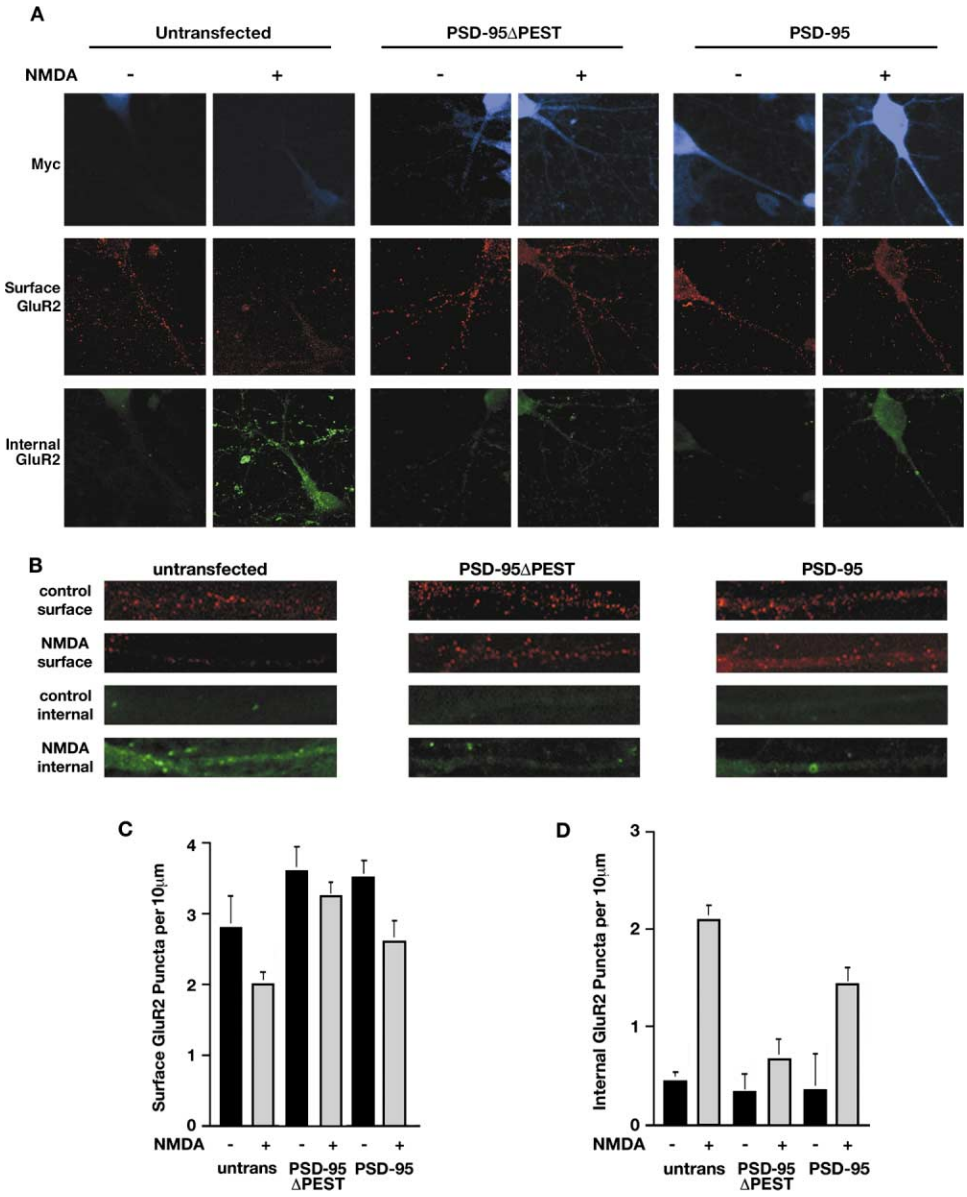

Figure 6. Ubiquitination of PSD-95 Regulates Endocytosis of AMPA Receptors

(A) (Top row) An antibody feeding technique was used to visualize endocytosed GluR2 in untransfected neurons (blue; left panels), neurons transfected with myc-PSD-95ΔPEST (blue; middle panels), or myc-tagged PSD-95 (blue; right panels). (Middle row) In untransfected neurons, NMDA treatment causes a loss of surface GluR2 staining (red; +; left panels). NMDA-induced loss of surface GluR2 is largely blocked in PSD-95ΔPEST-expressing neurons (red; middle panels) and blunted in neurons expressing wild-type PSD-95 (red; right panels). (Bottom row) In untransfected neurons (−; left panels), there is scant intracellular GluR2 staining (green). NMDA treatment (20 μM, 3 min) causes internalization of GluR2 (green; +; left panels). NMDA-induced GluR2 endocytosis was blocked in neurons expressing PSD-95ΔPEST (green; middle panels). NMDA-induced endocytosis of GluR2 was partially inhibited in neurons expressing wild-type PSD-95 (green; right panels). Background levels of myc antigen are faintly detected in the control neurons.

(B) Higher-magnification view of representative dendritic regions shows that in untransfected neurons (left column), NMDA treatment causes a loss of surface GluR2 (red) and a concomitant increase in intracellular GluR2 (green). In contrast, in neurons expressing PSD-95ΔPEST (middle column), the NMDA-induced loss of surface GluR2 (red) and increase in intracellular GluR2 (green) is largely attenuated. Both NMDA effects are blunted in neurons expressing wild-type PSD-95 (right columns).

(C) Quantification of the density of surface GluR2 puncta revealed untransfected, untreated control neurons had 2.6 ± 0.6 GluR2 puncta/10 μm ($n = 16$). Following NMDA treatment, untransfected neurons exhibited 1.9 ± 0.3 puncta per 10 μm ($p < 0.02$ versus control, $n = 16$). In neurons expressing PSD-95ΔPEST, GluR2 puncta density was 3.6 ± 0.4/10 μm ($n = 15$). NMDA treatment did not cause a significant decrease in density of surface GluR2 puncta (3.25 ± 0.2/10 μm, $p > 0.09$, $n = 15$). Neurons expressing wild-type PSD-95 had 3.5 ± 0.26 puncta/10 μm ($n = 16$). NMDA treatment reduced GluR2 puncta density to 2.6 ± 0.3/10 μm ($p < 0.05$, $n = 16$). Quanitatnion of data were performed using a double blind protocol.

(D) In untransfected neurons, NMDA treatment increased the density of internalized GluR2 puncta from 0.44 ± 0.1 puncta/10 μm to 2.1 ± 0.15 puncta/10 μm within 30 min ($n = 16$, $p < 0.01$). This NMDA-induced increase in internal GluR2 was blocked by transfection with PSD-95ΔPEST (control: internal GluR2 puncta was 0.33 ± 0.2 puncta/10 μm; $n = 15$; NMDA: internal GluR2 density was 0.68 ± 0.17/10 μm; $n = 15$, $p > 0.15$). In neurons expressing wild-type PSD-95, NMDA had a reduced effect compared to controls (0.36 ± 0.37 puncta/10 μm in untreated cells versus 1.44 ± 0.16 puncta/10 μm in NMDA treated cells; $n = 16$, $p < 0.05$). Quantitation of data were performed using a double blind protocol.

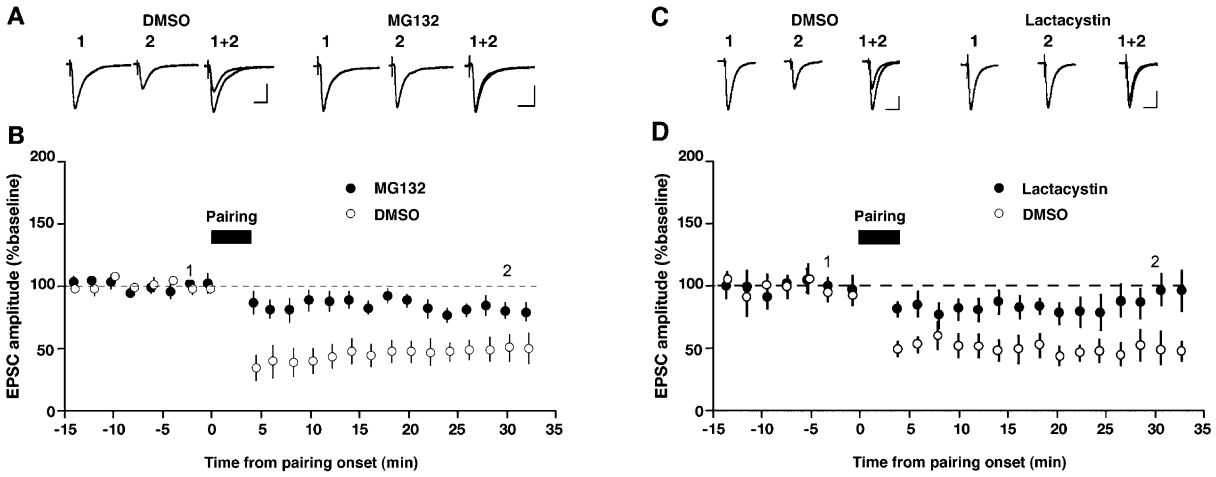

Figure 7. Inhibition of the Proteasome Reduces the Magnitude of Hippocampal LTD

(A and C) Sample EPSCs from a hippocampal slice illustrate the effect of MG132 (A) and lactacystin (C) on pairing-induced synaptic depression. CA1 pyramidal neurons were voltage-clamped at −65 mV. Following the pairing protocol, EPSCs were reduced by ~50% in DMSO vehicle control recordings. Inhibition of proteasome activity by MG132 (1 μM) and lactacystin (10 μM) significantly attenuated LTD. Sweeps are the average of consecutive responses taken 5 min prior to pairing onset (1) and 25–30 min following completion of the pairing protocol (2). All recordings were performed in the presence of the $GABA_A$ antagonist picrotoxin (50 μM). Scale bars, 50 pA, 30 ms (A); 25pA, 25 ms (C).

(B and D) Overlay of grouped data time courses demonstrates that MG132 (B) and lactacystin (D) attenuate LTD magnitude. Following 15 min of stable baseline recording, LTD was induced at time zero by a pairing protocol (black bar) and assessed 25–30 min after pairing. Proteasome inhibition by MG132 (●; n = 6) or lactacystin (●; n = 7) significantly reduced the magnitude of LTD compared to DMSO control (○; n = 6, 3 for panels [B] and [D], respectively). Plotted on the leftward *y* axis is EPSC amplitude normalized to a 15 min baseline period. Each symbol represents data averaged into 2 min bins.

modification of a major PSD component, the ubiquitin-proteasome pathway is critically involved in regulating synaptic strength and plasticity. The ideas are presented in a model (Figure 8).

Our pharmacological studies suggest that activation of the calcium-sensitive phosphatase PP2B may play a role in the ubiquitination/degradation of PSD-95 by Mdm2. During LTD, activation of PP2B initiates a signaling cascade that results in the dephosphorylation of synaptic PKA substrates (Beattie et al., 2000; Ehlers, 2000; Kameyama et al., 1998; Lee et al., 2000a; Lee et al., 1998). The GluR1 subunit of the AMPA receptor is one likely candidate substrate (Banke et al., 2000; Lee et al., 2000a; Tavalin et al., 2002). Interestingly, PP2B and PKA are targeted to AMPA receptors by the synaptic anchoring protein AKAP79/150 (Colledge et al., 2000). In this way, the enzymes are optimally positioned to regulate AMPA receptor phosphorylation and activity (Colledge et al., 2000; Oliveria et al., 2003; Rosenmund et al., 1994; Tavalin et al., 2002; M.L. Dell'Acqua, L.L. Gomez, S. Alam, A. Bishop, and J.D. Scott, 2001, Soc. Neurosci., abstract). Future studies are planned to examine a potential role for the AKAP79/150 signaling complex in coupling calcium signals to activation of a Mdm2/ubiquitin pathway.

Ubiquitination regulates synaptic strength, plasticity and structure in invertebrates and mammals (Burbea et al., 2002; Chain et al., 1999; DiAntonio et al., 2001; Ehlers, 2003; Hegde et al., 1997; Jiang et al., 1998; Speese et al., 2003; Wilson et al., 2002; Zhao et al., 2003). Recently,

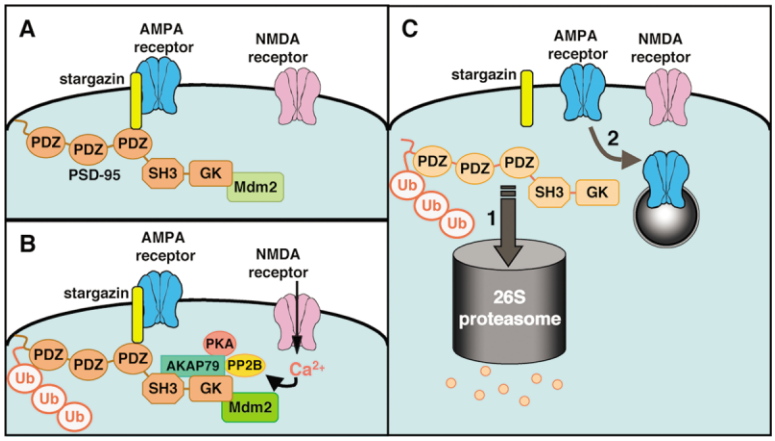

Figure 8. A Model for Ubiquitin-Mediated Regulation of Surface AMPA Receptors

(A) PSD-95 indirectly interacts with AMPA receptors through stargazin. In addition, PSD-95 also binds to Mdm2, a ubiquitin E3 ligase.

(B) In response to NMDA-induced calcium influx, PP2B is activated, and PSD-95 is rapidly ubiquitinated by associated Mdm2. PP2B and PKA may be targeted to the synapse through association with AKAP79/150.

(C) Following ubiquitination, PSD-95 is targeted to the proteasome where it is degraded (1). The loss of PSD-95 untethers AMPA receptors from the PSD, allowing endocytosis (2).

ubiquitination of *C. elegans* GLR-1 (a non-NMDA glutamate receptor subunit) was shown to regulate its abundance at synaptic sites (Burbea et al., 2002). Our data are consistent with a conserved role for ubiquitination in regulating the number of synaptic AMPA receptors in mammals—through degradation of their synaptic tethering protein PSD-95.

That two structurally distinct proteasome inhibitors (MG132 and lactacystin) both block PSD-95 degradation, and LTD strongly implicates a role for the proteasome in these processes. However, it is also possible that the lysosome may be involved in the regulation of PSD-95 stability and LTD. Although we did not detect ubiquitination of GluR2 in our experiments, our data do not rule out the possibility that other mammalian synaptic proteins, including AMPA receptor subunits themselves, also may be direct targets of the ubiquitin-proteasome system.

Indeed, recent work shows that long-term changes in synaptic activity can alter the levels of a variety of PSD proteins in cultured rat neurons through the ubiquitin-proteasome system (Ehlers, 2003). Of note is the fact that Ehlers did not observe ubiquitination of PSD-95. This is not surprising given that he screened for ubiquitinated proteins from unstimulated neurons (i.e., for proteins with a high basal level of ubiquitination). In fact, in our experiments, we observed ubiquitination of PSD-95 in cultured neurons only following NMDA stimulation (Figure 2A), consistent with Ehlers' data.

Recent reports have shown that the level of PSD-95 correlates with synaptic strength and maturation. Overexpression of PSD-95 enhances AMPA receptor-mediated synaptic transmission (Beique and Andrade, 2003; El-Husseini et al., 2000; Schnell et al., 2002) and increases the number and size of dendritic spines (El-Husseini et al., 2000). In contrast, removal of PSD-95 from the synaptic membrane downregulates AMPA receptor transmission (El-Husseini et al., 2002). Furthermore, PSD-95 mutant mice, which do not express synaptic PSD-95, also do not exhibit NMDA receptor-dependent LTD in the hippocampus (Migaud et al., 1998). Our data demonstrate a direct role for PSD-95 ubiquitination in the endocytosis of AMPA receptors. Overexpression of PSD-95ΔPEST—a mutant impaired in its ability to become ubiquitinated—dramatically reduces NMDA-stimulated endocytosis of AMPA receptors. In addition, we find that overexpression of wild-type PSD-95 partially reduces AMPA receptor endocytosis. We hypothesize that by interacting with AMPA receptors and other molecules in the PSD, PSD-95 stabilizes surface AMPA receptors. In support of this idea, previous studies have shown that association with PSD-95 prevents internalization of Kv1.4 and the β1-adrenergic receptor (Hu et al., 2000; Jugloff et al., 2000), indicating that when bound to PSD-95, associated receptors/channels may be prevented from undergoing endocytosis. By reducing ubiquitination, degradation, and loss of synaptic PSD-95, the ΔPEST mutant amplifies the effect of wild-type PSD-95.

In contrast to our data, El-Husseini et al. (2002) found that overexpression of wild-type PSD-95 increased glutamate-induced AMPA receptor internalization. We do not fully understand the reasons for the apparent discrepancy between this study and ours, but technical differences are likely to account, in part, for the differing results. In addition, recent studies have shown that overexpression of PSD-95 in hippocampal slices leads to an enhancement of LTD (Beique and Andrade, 2003; Stein et al., 2003). Clearly, future studies are required to understand the precise role PSD-95 plays in synaptic plasticity. It will be interesting to test the effects of ubiquitination-deficient mutants of PSD-95 on hippocampal synaptic plasticity.

The data in this report suggest that ubiquitination and degradation of PSD-95 may be a molecular mechanism underlying dynamic changes in AMPA receptor levels at the synapse. Recent work showing that eye opening causes the rapid redistribution of PSD-95 to dendrites in visual neurons (Yoshii et al., 2003) provides further support for a role for PSD-95 in activity-dependent synaptic changes. Given that ubiquitination plays a role in several forms of mammalian memory (Jiang et al., 1998; Lopez-Salon et al., 2001; Moss et al., 2002), future studies should focus on a role for ubiquitination and degradation of PSD-95 in memory formation and stability.

Experimental Procedures

Expression Constructs

The myc-tagged PSD-95 construct in GW1-CMV was a gift from Morgan Sheng, the HA-ubiquitin construct in pCMV was a gift of Dirk Bohmann, and the myc-tagged p14ARF construct in pCDNA3 was a gift of Yanping Zhang. Construction of the GST fusions proteins of PSD-95 domains has been described (Colledge et al., 2000). PSD-95ΔPEST mutant was generated by QuikChange Site-Directed mutagenesis (Stratagene); primers were designed to delete amino acids 10–25 of rat PSD-95.

Antibodies

Antibodies used in immunoprecipitation experiments included Mdm2 (Santa Cruz Biotechnology; rabbit polyclonal sc-7918); E6AP (Affinity Bioreagents; rabbit polyclonal PA3-843); Parkin (Cell Signaling Technologies; rabbit polyclonal #2132); Cbl (Santa Cruz; rabbit polyclonal sc-170); GluR1 (Upstate Biotechnology; rabbit peptide 06-306); AKAP150 (ICOS; rabbit polyclonal clone 4361J); and NR1 (Upstate; rabbit polyclonal 06-311). For Western blots, the following antibodies were used: ubiquitin (BD Pharmingen; mouse monoclonal 6C1.17; 1:2000); HA (Sigma; rabbit peptide H6903; 1:1000); PSD-95 (Upstate; mouse monoclonal K28/43; 1:10,000); myc (Santa Cruz; mouse monoclonal 9E10; 1:2000); Mdm2 (mouse monoclonal 4B11 (Chen et al., 1993; 1:1000). In all cases, Western blots shown are representative examples of experiments that were performed at least three times.

Brain Extract Preparation

For immunoprecipitation of PSD-95-Mdm2 complexes, extracts of rat forebrain crude synaptosomes were prepared by solubilization in deoxycholic acid according to described procedures (Dunah et al., 1998). Briefly, forebrain P2 fraction was extracted in 1% deoxycholic acid and dialyzed overnight against 0.1% Triton X-100 and 50 mM Tris (pH 7.4). Following centrifugation at 38,000 × *g* for 30 min at 4°C, 100 μg of supernatant was incubated with 1–3 μg of antibody and 30 μl of prewashed protein A or G sepharose (50% slurry) overnight at 4°C. Following washing, bound proteins were eluted with SDS-sample buffer, separated by SDS-PAGE on a 4%–15% gradient gel (Biorad), transferred to nitrocellulose membrane. Immunoreactive bands were visualized by enhanced chemiluminescence (ECL; Amersham or Pierce) and captured on autoradiography film (Amersham Hyperfilm ECL or Kodak Biomax film).

Transfection of Heterologous Cells

HEK293 cells were transfected at 60%–80% confluency in 10 cm^2 plates using the calcium phosphate method. H1299 and MEFs were transfected by Lipofectamine (Invitrogen). One to four μg of each

cDNA construct was transfected per dish. Cells were harvested and lysed 24 hr after transfection in 500 μl RIPA buffer (1% Triton X-100, 0.1% SDS, 0.5% deoxycholic acid, 50 mM $NaPO_4$, 150 mM NaCl, 2 mM EDTA and protease inhibitors). Cell extracts were analyzed directly or were subjected to immunoprecipitation using 1–3 μg antibody and 30 μl of protein A or G Sepharose. Following overnight incubation at 4°C, the immunoprecipitates were washed and bound proteins were analyzed by immunoblotting. Digital images, produced by densitometric scans of autoradiographs on a ScanJet IIcx (Hewlett Packard, Palo Alto, California) with DeskScan II software (Hewlett Packard), were quantified using NIH Image 1.60 software.

In Vitro Ubiquitination Assay

The PSD-95 in vitro ubiquitination assay was performed as described previously (Honda et al., 1997) with some modifications. The assay was carried out in a 20 μl reaction mixture containing 50 mM Tris-HCl (pH 8.0), 5 mM $MgCl_2$, 0.5 mM DTT, 2 mM NaF, 3 μM okadaic acid, 100 ng GST-PSD-95, 100 ng MDM2, 200 ng UBA-1200 ng UBC-5, 500 ng HA-ubiquitin, 5 mM ATP (Pharmacia Biotech), 1.5 mM ATPγS (Fisher ICN). In control reactions, 100 ng His-p53 or 100 ng GST were used in place of GST-PSD-95. The mixture was incubated at 37°C for 60 min and then analyzed by SDS-PAGE. Ubiquitinated GST-PSD-95 was detected with anti-PSD-95 antibody (Upstate Biotechnology; clone K28/43; 1:10,000).

Dissociated Hippocampal Neuron Culture

All rats were housed either in the Brown University Animal Care Facility or Vollum Institute Animal Care Facility, and all procedures were approved by institutional animal care and use committees. The hippocampus was removed from P0-P2 rats, exposed to papain (20 U/ml) at 37°C for 60 min, and dissociated by trituration. Cells were plated onto poly-lysine-coated (1 mg/ml) glass-bottomed dishes. For immunocytochemistry, cells were plated at 75,000 cells/ml (1.5 ml/dish); for biochemistry, cells were plated at 500,000 cells/ml. Cultures were grown in media containing DMEM with 5% fetal bovine serum, 4 mM L-glutamine, B-27 nutrient supplement, penicillin (5 U/ml), and streptomycin (5 μg/ml). For immunoprecipitation of PSD-95 and GluR2, neurons were lysed in RIPA buffer (0.1% SDS, 0.5% deoxycholic acid, 1% Triton X-100, 50 mM $NaPO_4$, 150 mM NaCl, 2 mM EDTA, and protease inhibitors).

Immunocytochemistry

Following experimental treatment, low-density neuronal cultures were fixed in 4% paraformaldehyde with 4% sucrose for 5 min. Neurons were incubated in blocking buffer (20% fetal bovine serum in PBS) for 1 hr and then exposed to antibodies against synapsin 1 (1:1000; Chemicon), Mdm2 (1:100; Santa Cruz), or PSD-95 (1:200; MA1-045/046 Affinity Bioreagents) overnight at 4°C in blocking buffer. Cultures were then rinsed in blocking buffer containing 0.1% Triton-X-100 for 20 min, exposed to the appropriate fluorescent secondary antibodies (Jackson Immunoresearch) for 1 hr, and mounted in Vectashield. Omission of primary antibody was used as a control for specificity of staining and showed only faint background staining.

For surface label of AMPA receptors, neuronal cultures were placed on ice to inhibit endocytosis, and surface receptors were labeled with GluR2 antibodies directed against an extracellular epitope (Chemicon; MAB397; 1:100) for 30 min. Cultures were rinsed twice for 15 min in PBS, fixed in 4% paraformaldehyde with 4% sucrose for 5 min, and blocked in PBS containing 10% normal goat serum for 1 hr. For PSD-95 transfection experiments, cultures were permeabilized with 0.25% Triton-X-100 and stained overnight at 4°C with rabbit polyclonal antibodies directed against the myc tag (Upstate Biotechnology; 1:200) to identify PSD-95-transfected cells. Cultures were rinsed in blocking buffer two times 20 min at room temperature and exposed to the appropriate fluorescent secondary antibodies (Jackson Immunoresearch; 1:300) in blocking buffer overnight at 4°C. Cultures were rinsed three times 20 min and cover slipped in Vectashield (Vector Laboratories). Cultures were examined on a Olympus Fluoview 300 laser scanning confocal microscope with experimenters blind to culture history. Images were collected using Fluoview software and converted to NIH image files.

For quantification of PSD-95, GluR2, and Mdm2 staining, puncta were defined as regions of staining intensity twice that of background on dendrite. Synaptic puncta were defined as regions of staining overlapping synapsin 1 puncta. Puncta were delineated manually in NIH image (average synaptic diameter 1.5 μm), and average pixel intensity was measured.

Transfection of Primary Neuronal Cultures and Immunocytochemical Measurement of Endocytosis

Primary hippocampal cultures were transfected using the calcium phosphate method (Xia et al., 1996) at 5 days in vitro (DIV). Endocytosis of AMPA receptors was examined at14 DIV using the antibody feeding protocol (Ehlers, 2000; Lin et al., 2000). Surface GluR2 receptors were labeled on living neurons (Chemicon MAB397; 1:200) at 37°C for 30 min, prior to treatment with NMDA (20 μM, 3 min). Cultures were immediately rinsed and returned to the incubator for an additional 27 min to allow endocytosis to occur. Cultures were then fixed in 4% paraformaldehyde, 4% sucrose. Surface AMPA receptors were labeled with Alexa-568-conjugated (red) anti-mouse secondary antibodies for 2 hr (1:250; data not shown). Cultures were then permeabilized for 1 min with 100% methanol and stained with Alexa 488-conjugated (green) anti-mouse secondary antibody to label internalized AMPA receptors. To visualize PSD-95-transfected neurons, cultures were labeled with anti-myc antibodies and Alexa-633-conjugated (blue) anti-rabbit secondary antibodies.

Biochemical Measurements of Surface Receptor Levels

Methods for biotinylation experiments were previously described (Snyder et al., 2001). Following treatment, 7- to 14-day-old high-density cultured neurons were placed on ice to halt receptor trafficking and washed twice with ice-cold artificial cerebrospinal fluid (ACSF; 124 mM NaCl, 5 mM KCl, 1.25 mM NaH_2PO_4, 26 mM $NaHCO_3$, 0.8 mM $MgCl_2$, 1.8 mM $CaCl_2$, 10 mM dextrose, saturated with 95% O_2 and 5% CO_2.) Cultures were then incubated with ACSF containing 1 mg/ml Sulfo-NHS-LC-Biotin (Pierce Chemical Company) for 30 min on ice. Cultures were rinsed in Tris buffered saline (TBS) to quench the biotin reaction. Cultures were lysed in 300 μl of RIPA buffer. The homogenates were centrifuged at 14,000 × *g* for 15 min at 4°C. The supernatant (200 μl) was incubated with 100 μl of 50% neutravidin agarose beads (Pierce Chemical Company) for 3 hr or overnight at 4°C. Neutravidin-bound proteins were washed three times with RIPA buffer and resuspended in 40 μl of SDS sample buffer and boiled. Quantitative Western blots were performed on biotinylated (surface) proteins using anti-GluR1 C-terminal (1:1000; Upstate Biotechnology); transferrin receptor antibodies (TfR; monoclonal clone H68.4; 1:1000 [0.5 μg/ml]; Zymed Laboratories). Previous control experiments confirmed that the intracellular protein actin was not biotinylated in this assay (n = 3).

Electrophysiology

Long-Evans rats aged P14–P20 (Charles River) were deeply anesthetized with an injection of D-beuthanasia. Following the disappearance of corneal reflexes and a tail pinch response, the rat was decapitated according to U.S. Department of Health and Human Services and Brown University animal care guidelines. The brain was rapidly removed and placed into ice-cold dissection buffer consisting of 212 mM sucrose, 10 mM glucose, 2.6 mM KCl, 1.23 mM NaH_2PO_4, 26 mM $NaHCO_3$, 9 mM $MgCl_2$, and 1 mM $CaCl_2$. Slices of ventral hippocampus (350 μm) were obtained using a vibrating-blade microtome (Leica VT1000S), and connections from CA3 and subiculum were severed to prevent epileptiform activity. Slices were transferred to a holding chamber containing ACSF that consisted of 124 mM NaCl, 2.5 mM KCl, 2 mM $CaCl_2$, 1 mM $MgCl_2$, 1.23 mM NaH_2PO_4, 26 mM $NaHCO_3$, and 10 mM dextrose. Slices were allowed to recover at room temperature for a minimum of 1 hr prior to recording.

For recordings, a slice was transferred to a submersion-type recording chamber and perfused with room temperature (25°C), oxygenated ACSF that also contained 50 μM picrotoxin to inhibit $GABA_A$ responses. Individual CA1 pyramidal neurons were visualized with an inverted microscope (Nikon) outfitted with a 40×, 0.8 numerical aperture objective and IR-DIC optics. Whole-cell voltage-clamp recordings were performed using patch pipettes made of thick-walled glass (Sutter, 1.5 mm O.D., 0.86 mm I.D.) and filled with internal

solution containing 107 mM D-gluconic acid, 107 mM CsOH, 5 mM QX-314 chloride, 0.2 mM EGTA, 20 mM HEPES, 3.7 mM NaCl, 4 mM Mg-ATP, 0.3 mM Na-GTP, with pH adjusted to 7.2. Pipette resistances were 3–5 MΩ. EPSCs were recorded with an Axopatch 200B amplifier (Axon Instruments), and data were acquired and analyzed using a system from DataWave Technologies (Boulder, CO) or pClamp 9 software and digidata 1332 digitizer (Union City, CA). Experiments were included in the data set if the baseline period was stable, series resistance was stable ($<\pm$10%) for the recording duration, and monosynaptic EPSCs were evoked. Further, experiments were excluded if Rs $>$ 35 MΩ. There were no significant differences in the average series resistances for MG132 or DMSO control groups (20.2 $\pm$ 3.8 and 16.0 $\pm$ 1.2 MΩ, respectively; $p > 0.3$). EPSCs were elicited by delivering 100 μs current pulses with a 2-contact cluster electrode (FHC, 2 $\times$ 25 μm Pt/Ir) placed in stratum radiatum. Test stimuli were delivered at 0.33 Hz, and stimulation intensity was titrated to elicit reliably a monosynaptic EPSC with few failures. The test potential for all recordings was −65 mV. LTD was induced by pairing 1 Hz stimulation with membrane depolarization to −40 mV for 200 pulses (Selig et al., 1995). For statistical comparisons of LTD, the EPSC peak amplitude was normalized to the average of a 15 min baseline period prior to the onset of the pairing protocol and then compared to a 5 min period beginning 25 min following the completion of the pairing protocol. The proteasome inhibitor MG132 (Calbiochem) was dissolved in DMSO, stored as a stock solution at 10 mM at −20°C for no more than 1 month. The MG132 stock solution was diluted 1:10,000 in internal solution to yield a final concentration of 1 μM. Lactacystin (Calbiochem) was prepared as a stock solution at 10 mM and used at 10 μM. MG132 and lactacystin experiments were interleaved with DMSO vehicle controls (0.01% by volume). QX-314 chloride was purchased from Alomone Labs (Israel). All other reagents were from Sigma.

Statistical Analysis

For statistical analysis of time courses (Figures 1D, 5F, and 5G), one-way analysis of variance (ANOVA) with Bonferoni post hoc comparisons were made. For analysis of LTD time courses (Figure 7), ANOVA followed by Fisher's PLSD post hoc tests were used with significance placed at $p < 0.05$. In all other cases, statistical comparisons were made using unpaired t tests with significance placed at $p < 0.05$ and data are expressed as mean $\pm$ SEM. Statistics were performed using StatView or Prism 3.0 software.

Acknowledgments

We thank Dr. Mathew Thayer (OHSU) for Mdm2 constructs, Dr. Dirk Bohmann (EMBL, Heidelberg, Germany) for the HA-ubiquitin construct, Dr. Morgan Sheng (MIT) for the PSD-95 construct, and Dr. Yanping Zhang for the p14ARF construct. We thank Mushui Dai for generation and purification of Mdm2. We thank Robert Mouton, Nicole Bonnett, and Ian Townley for providing cell culture assistance. We are grateful to members of the Scott and Bear labs for their support and advice during this work. In particular, we appreciate the advice of Dr. Jennifer Michel. This work was supported by NIH grants GM48231 to J.D.S. and NS39321 to M.F.B. and from a CIHR grant to M.C.

Received: February 26, 2003
Revised: September 16, 2003
Accepted: October 15, 2003
Published: October 29, 2003

References

Banke, T.G., Bowie, D., Lee, H., Huganir, R.L., Schousboe, A., and Traynelis, S.F. (2000). Control of GluR1 AMPA receptor function by cAMP-dependent protein kinase. J. Neurosci. *20*, 89–102.

Bear, M.F., and Malenka, R.C. (1994). Synaptic plasticity: LTP and LTD. Curr. Opin. Neurobiol. *4*, 389–399.

Beattie, E.C., Carroll, R.C., Yu, X., Morishita, W., Yasuda, H., von Zastrow, M., and Malenka, R.C. (2000). Regulation of AMPA receptor endocytosis by a signaling mechanism shared with LTD. Nat. Neurosci. *3*, 1291–1300.

Beique, J.C., and Andrade, R. (2003). PSD-95 regulates synaptic transmission and plasticity in rat cerebral cortex. J. Physiol. *546*, 859–867.

Burbea, M., Dreier, L., Dittman, J.S., Grunwald, M.E., and Kaplan, J.M. (2002). Ubiquitin and AP180 regulate the abundance of GLR-1 glutamate receptors at postsynaptic elements in *C. elegans*. Neuron *35*, 107–120.

Carroll, R.C., Beattie, E.C., Xia, H., Luscher, C., Altschuler, Y., Nicoll, R.A., Malenka, R.C., and von Zastrow, M. (1999). Dynamin-dependent endocytosis of ionotropic glutamate receptors. Proc. Natl. Acad. Sci. USA *96*, 14112–14117.

Chain, D.G., Schwartz, J.H., and Hegde, A.N. (1999). Ubiquitin-mediated proteolysis in learning and memory. Mol. Neurobiol. *20*, 125–142.

Chen, J., Marechal, V., and Levine, A.J. (1993). Mapping of the p53 and mdm-2 interaction domains. Mol. Cell. Biol. *13*, 4107–4114.

Chen, L., Chetkovich, D.M., Petralia, R.S., Sweeney, N.T., Kawasaki, Y., Wenthold, R.J., Bredt, D.S., and Nicoll, R.A. (2000). Stargazin regulates synaptic targeting of AMPA receptors by two distinct mechanisms. Nature *408*, 936–943.

Colledge, M., Dean, R.A., Scott, G.K., Langeberg, L.K., Huganir, R.L., and Scott, J.D. (2000). Targeting of PKA to glutamate receptors through a MAGUK-AKAP complex. Neuron *27*, 107–119.

DiAntonio, A., Haghighi, A.P., Portman, S.L., Lee, J.D., Amaranto, A.M., and Goodman, C.S. (2001). Ubiquitination-dependent mechanisms regulate synaptic growth and function. Nature *412*, 449–452.

Dunah, A.W., Luo, J., Wang, Y.H., Yasuda, R.P., and Wolfe, B.B. (1998). Subunit composition of N-methyl-D-aspartate receptors in the central nervous system that contain the NR2D subunit. Mol. Pharmacol. *53*, 429–437.

Ehlers, M.D. (2000). Reinsertion or degradation of AMPA receptors determined by activity-dependent endocytic sorting. Neuron *28*, 511–525.

Ehlers, M.D. (2003). Activity level controls postsynaptic composition and signaling via the ubiquitin-proteasome system. Nat. Neurosci. *10*, 10.

El-Husseini, A.E., Schnell, E., Chetkovich, D.M., Nicoll, R.A., and Bredt, D.S. (2000). PSD-95 involvement in maturation of excitatory synapses. Science *290*, 1364–1368.

El-Husseini, A.E., Schnell, E., Dakoji, S., Sweeney, N., Zhou, Q., Prange, O., Gauthier-Campbell, C., Aguilera-Moreno, A., Nicoll, R.A., and Bredt, D.S. (2002). Synaptic strength regulated by palmitate cycling on PSD-95. Cell *108*, 849–863.

Gardiol, D., Kuhne, C., Glaunsinger, B., Lee, S.S., Javier, R., and Banks, L. (1999). Oncogenic human papillomavirus E6 proteins target the discs large tumour suppressor for proteasome-mediated degradation. Oncogene *18*, 5487–5496.

Glaunsinger, B.A., Lee, S.S., Thomas, M., Banks, L., and Javier, R. (2000). Interactions of the PDZ-protein MAGI-1 with adenovirus E4–ORF1 and high- risk papillomavirus E6 oncoproteins. Oncogene *19*, 5270–5280.

Hegde, A.N., and DiAntonio, A. (2002). Ubiquitin and the synapse. Nat. Rev. Neurosci. *3*, 854–861.

Hegde, A.N., Inokuchi, K., Pei, W., Casadio, A., Ghirardi, M., Chain, D.G., Martin, K.C., Kandel, E.R., and Schwartz, J.H. (1997). Ubiquitin C-terminal hydrolase is an immediate-early gene essential for long-term facilitation in Aplysia. Cell *89*, 115–126.

Heynen, A.J., Quinlan, E.M., Bae, D.C., and Bear, M.F. (2000). Bidirectional, activity-dependent regulation of glutamate receptors in the adult hippocampus in vivo. Neuron *28*, 527–536.

Honda, R., Tanaka, H., and Yasuda, H. (1997). Oncoprotein MDM2 is a ubiquitin ligase E3 for tumor suppressor p53. FEBS Lett. *420*, 25–27.

Hu, L.A., Tang, Y., Miller, W.E., Cong, M., Lau, A.G., Lefkowitz, R.J., and Hall, R.A. (2000). beta 1-adrenergic receptor association with PSD-95. Inhibition of receptor internalization and facilitation of beta 1-adrenergic receptor interaction with N-methyl-D-aspartate receptors. J. Biol. Chem. *275*, 38659–38666.

Jiang, Y.H., Armstrong, D., Albrecht, U., Atkins, C.M., Noebels, J.L., Eichele, G., Sweatt, J.D., and Beaudet, A.L. (1998). Mutation of the

Angelman ubiquitin ligase in mice causes increased cytoplasmic p53 and deficits of contextual learning and long-term potentiation. Neuron *21*, 799–811.

Joazeiro, C.A., and Hunter, T. (2000). Biochemistry. Ubiquitination–more than two to tango. Science *289*, 2061–2062.

Jugloff, D.G., Khanna, R., Schlichter, L.C., and Jones, O.T. (2000). Internalization of the Kv1.4 potassium channel is suppressed by clustering interactions with PSD-95. J. Biol. Chem. *275*, 1357–1364.

Kameyama, K., Lee, H.K., Bear, M.F., and Huganir, R.L. (1998). Involvement of a postsynaptic protein kinase A substrate in the expression of homosynaptic long-term depression. Neuron *21*, 1163–1175.

Lee, H.K., Kameyama, K., Huganir, R.L., and Bear, M.F. (1998). NMDA induces long-term synaptic depression and dephosphorylation of the GluR1 subunit of AMPA receptors in hippocampus. Neuron *21*, 1151–1162.

Lee, H.K., Barbarosie, M., Kameyama, K., Bear, M.F., and Huganir, R.L. (2000a). Regulation of distinct AMPA receptor phosphorylation sites during bidirectional synaptic plasticity. Nature *405*, 955–959.

Lee, S.S., Glaunsinger, B., Mantovani, F., Banks, L., and Javier, R.T. (2000b). Multi-PDZ domain protein MUPP1 is a cellular target for both adenovirus E4–ORF1 and high-risk papillomavirus type 18 E6 oncoproteins. J. Virol. *74*, 9680–9693.

Liao, D., Zhang, X., O'Brien, R., Ehlers, R.O., and Huganir, R.L. (1999). Regulation of morphological postsynaptic silent synapses in developing hippocampal neurons. Nat. Neurosci. *2*, 37–43.

Lin, J.W., Ju, W., Foster, K., Lee, S.H., Ahmadian, G., Wyszynski, M., Wang, Y.T., and Sheng, M. (2000). Distinct molecular mechanisms and divergent endocytotic pathways of AMPA receptor internalization. Nat. Neurosci. *3*, 1282–1290.

Liu, J., Farmer, J.D., Jr., Lane, W.S., Friedman, J., Weissman, I., and Schreiber, S.L. (1991). Calcineurin is a common target of cyclophilin-cyclosporin A and FKBP-FK506 complexes. Cell *66*, 807–815.

Lopez-Salon, M., Alonso, M., Vianna, M.R., Viola, H., Mello e Souza, T., Izquierdo, I., Pasquini, J.M., and Medina, J.H. (2001). The ubiquitin-proteasome cascade is required for mammalian long-term memory formation. Eur. J. Neurosci. *14*, 1820–1826.

Lu, W., Man, H., Ju, W., Trimble, W.S., MacDonald, J.F., and Wang, Y.T. (2001). Activation of synaptic NMDA receptors induces membrane insertion of new AMPA receptors and LTP in cultured hippocampal neurons. Neuron *29*, 243–254.

Lüscher, C., Xia, H., Beattie, E.C., Carroll, R.C., von Zastrow, M., Malenka, R.C., and Nicoll, R.A. (1999). Role of AMPA receptor cycling in synaptic transmission and plasticity. Neuron *24*, 649–658.

Malinow, R., and Malenka, R.C. (2002). AMPA receptor trafficking and synaptic plasticity. Annu. Rev. Neurosci. *25*, 103–126.

Man, H.-Y., Lin, J.W., Ju, W.H., Ahmadian, G., Liu, L., Becker, L.E., Sheng, M., and Wang, Y.T. (2000). Regulation of AMPA receptor-mediated synaptic transmission by clathrin-dependent receptor internalization. Neuron *25*, 649–662.

Migaud, M., Charlesworth, P., Dempster, M., Webster, L.C., Watabe, A.M., Makhinson, M., He, Y., Ramsay, M.F., Morris, R.G., Morrison, J.H., et al. (1998). Enhanced long-term potentiation and impaired learning in mice with mutant postsynaptic density-95 protein. Nature *396*, 433–439.

Montes de Oca Luna, R., Wagner, D.S., and Lozano, G. (1995). Rescue of early embryonic lethality in mdm2-deficient mice by deletion of p53. Nature *378*, 203–206.

Moss, A., Blackburn-Munro, G., Garry, E.M., Blakemore, J.A., Dickinson, T., Rosie, R., Mitchell, R., and Fleetwood-Walker, S.M. (2002). A role of the ubiquitin-proteasome system in neuropathic pain. J. Neurosci. *22*, 1363–1372.

Mulkey, R.M., Endo, S., Shenolikar, S., and Malenka, R.C. (1994). Involvement of a calcineurin/inhibitor-1 phosphatase cascade in hippocampal long-term depression. Nature *369*, 486–488.

Murphey, R.K., and Godenschwege, T.A. (2002). New roles for ubiquitin in the assembly and function of neuronal circuits. Neuron *36*, 5–8.

Oliveria, S.F., Gomez, L.L., and Dell'Acqua, M.L. (2003). Imaging kinase–AKAP79–phosphatase scaffold complexes at the plasma membrane in living cells using FRET microscopy. J. Cell Biol. *160*, 101–112.

Pickart, C.M. (2000). Ubiquitin in chains. Trends Biochem. Sci. *25*, 544–548.

Rechsteiner, M., and Rogers, S.W. (1996). PEST sequences and regulation by proteolysis. Trends Biochem. Sci. *21*, 267–271.

Rosenmund, C., Carr, D.W., Bergeson, S.E., Nilaver, G., Scott, J.D., and Westbrook, G.L. (1994). Anchoring of protein kinase A is required for modulation of AMPA/kainate receptors on hippocampal neurons. Nature *368*, 853–856.

Schnell, E., Sizemore, M., Karimzadegan, S., Chen, L., Bredt, D.S., and Nicoll, R.A. (2002). Direct interactions between PSD-95 and stargazin control synaptic AMPA receptor number. Proc. Natl. Acad. Sci. USA *99*, 13902–13907.

Selig, D.K., Hjelmstad, G.O., Herron, C., Nicoll, R.A., and Malenka, R.C. (1995). Independent mechanisms for long-term depression of AMPA and NMDA responses. Neuron *15*, 417–426.

Sheng, M. (2001). Molecular organization of the postsynaptic specialization. Proc. Natl. Acad. Sci. USA *98*, 7058–7061.

Sherr, C.J., and Weber, J.D. (2000). The ARF/p53 pathway. Curr. Opin. Genet. Dev. *10*, 94–99.

Shi, S., Hayashi, Y., Esteban, J.A., and Malinow, R. (2001). Subunit-specific rules governing AMPA receptor trafficking to synapses in hippocampal pyramidal neurons. Cell *105*, 331–343.

Snyder, E.M., Philpot, B.D., Huber, K.M., Dong, X., Fallon, J.R., and Bear, M.F. (2001). Internalization of ionotropic glutamate receptors in response to mGluR activation. Nat. Neurosci. *4*, 1079–1085.

Speese, S.D., Trotta, N., Rodesch, C.K., Aravamudan, B., and Broadie, K. (2003). The ubiquitin proteasome system acutely regulates presynaptic protein turnover and synaptic efficacy. Curr. Biol. *13*, 899–910.

Stein, V., House, D.R.C., Bredt, D.S., and Nicoll, R.A. (2003). Postsynaptic Density-95 mimics and occludes hippocampal long-term potentiation and enhances long-term depression. J. Neurosci. *23*, 5503–5506.

Tavalin, S.J., Colledge, M., Hell, J.W., Langeberg, L.K., Huganir, R.L., and Scott, J.D. (2002). Regulation of GluR1 by the A-kinase anchoring protein 79 (AKAP79) signaling complex shares properties with long-term depression. J. Neurosci. *22*, 3044–3051.

Weissman, A.M. (2001). Themes and variations on ubiquitylation. Nat. Rev. Mol. Cell Biol. *2*, 169–178.

Wilson, S.M., Bhattacharyya, B., Rachel, R.A., Coppola, V., Tessarollo, L., Householder, D.B., Fletcher, C.F., Miller, R.J., Copeland, N.G., and Jenkins, N.A. (2002). Synaptic defects in ataxia mice result from a mutation in Usp14, encoding a ubiquitin-specific protease. Nat. Genet. *32*, 420–425.

Xia, Z., Dudek, H., Miranti, C.K., and Greenberg, M.E. (1996). Calcium influx via the NMDA receptor induces immediate early gene transcription by a MAP kinase/ERK-dependent mechanism. J. Neurosci. *16*, 5425–5436.

Yoshii, A., Sheng, M.H., and Constantine-Paton, M. (2003). Eye opening induces a rapid dendritic localization of PSD-95 in central visual neurons. Proc. Natl. Acad. Sci. USA *100*, 1334–1339.

Zeng, H., Chattarji, S., Barbarosie, M., Rondi-Reig, L., Philpot, B.D., Miyakawa, T., Bear, M.F., and Tonegawa, S. (2001). Forebrain-specific calcineurin knockout selectively impairs bidirectional synaptic plasticity and working/episodic-like memory. Cell *107*, 617–629.

Zhao, Y., Hegde, A.N., and Martin, K.C. (2003). The ubiquitin proteasome system functions as an inhibitory constraint on synaptic strengthening. Curr. Biol. *13*, 887–898.